SDEE-Faisal-etal-2013

by Ade Faisal

Submission date: 20-Nov-2018 09:06PM (UTC+0700)
Submission ID: 1042567014
File name: SDEE-Faisal-etal-2013.docx (673.35K)
Word count: 8666
Character count: 47230

Soil Dynamics and Earthquake Engineering 44 (2013) 42–53

Contents lists available at SciVerse ScienceDirect

Soil Dynamics and Earthquake Engineering

journal homepage: www.elsevier.com/locate/soildyn

Investigation of story ductility demands of inelastic concrete frames subjected to repeated earthquakes

Ade Faisal [a], Taksiah A. Majid [b,n], George D. Hatzigeorgiou [c]

[a] Fakultas Teknik, Universitas Muhammadiyah Sumatera Utara, Medan, Indonesia
[b] Disaster Research Nexus, School of Civil Engineering, Universiti Sains Malaysia, 14300 Nibong Tebal, P. Pinang, Malaysia
[c] Department of Environmental Engineering, Democritus University of Thrace, Xanthi, Greece

article info

Article history:
Received 18 January 2012
Received in revised form
9 June 2012
Accepted 19 August 2012
Available online 29 September 2012

abstract

The present study focuses on the influence of repeated earthquakes on the maximum story ductility demands of three-dimensional inelastic concrete frames. A comprehensive assessment is conducted using generic frames with 3-, 6-, 12-, and 18-story structures. Each is assumed to have behaviour factors of 1.5, 2, 4, and 6 referring to Eurocode 8. Stiffness and strength degrading hysteresis rule to represent reinforced concrete structure is considered in the plastic hinge of members. Twenty ground motions are selected, and single, double, and triple events of synthetic repeated earthquakes are considered. Some interesting findings are provided showing that repeated earthquakes significantly increase the story ductility demand of inelastic concrete frames. On average, relative increment of maximum story ductility demand is experienced 1.4 and 1.3 times when double and triple events of repeated earthquakes are induced, respectively. Empirical relationships are also provided to predict these increments where their efficiency is presented examining characteristic 3- and 8-story reinforced concrete buildings.

1. Introduction

Earthquakes do not usually occur as a single event, as mostly assumed in seismic design, but as a series of shocks. Strong earthquakes have more and larger aftershocks, as well as foreshocks, and the sequences can last for years or even longer. Aftershocks are usually unpredictable and can be of large magnitude, which could collapse buildings damaged from the main shock. Repetition of medium-strength earthquake ground motions ground motions after intervals of time characterizes repeated earthquakes [1]. The interval of time can be short or long, taking several minutes, hours, days, or even years, but not more than the structure lifetime (i.e., 50 years). The combination of foreshock, mainshock, and aftershock in repeated earthquakes is illustrated in Fig. 1 and listed in Table 1. These data explain that repeated earthquakes are not a series of foreshock, mainshock, and aftershock within a 24 h period only. Furthermore, repeated earthquakes are not necessarily sourced from the same ruptured fault because it can be experienced by sites situated near active faults having various fault types and rupture mechanism (e.g., Tarzana, Los Angeles). Repeated earthquakes can be a combination of near- and far-field earthquakes containing ground motions with forward directivity (pulse) and backward directivity (no pulse) effects.

In such cases of repeated earthquakes, structures already damaged after the first earthquake ground motion and remaining unrepaired may become completely inadequate at the end of the repeated earthquakes [4]. Despite evidence that repeated earthquakes hazard is clearly threatening, the effect of repeated earthquakes on the structures has not attracted much attention [5]. To the best of the authors' knowledge, only a few studies have examined the repeated earthquakes effects on buildings. Recent studies published addressed the needs in engineering design and evaluation with some constraints. For instance, some of the studies focused on the response of single-of-degree-freedom (SDOF) systems having bilinear elastoplastic hysteresis with no stiffness and strength degradation [5–7]. In fact, real structures can be efficiently simulated with multi-degree-of-freedom (MDOF) systems comprising beams, columns, and beam–column joints those can be deformed in different manners due to cyclic loading reversals propagated by earthquake ground motion. For instance, the story ductility, as a product of interstory drift, is more sensitive than the global ductility in detecting structural damage of elements resulting from roof drift. The story ductility is also directly linked to the level of inelastic behaviour that the system experiences [8]. Moreover, the effect of having hysteresis model with stiffness degradation on the peak displacement of short period of structures is apparently significant and

* Corresponding author. Tel.: þ604 5996283x6292; fax: þ604 5941009.
E-mail address: taksiah@eng.usm.my (T.A. Majid).

0267-7261/$ - see front matter & 2012 Elsevier Ltd. All rights reserved.
http://dx.doi.org/10.1016/j.soildyn.2012.08.012

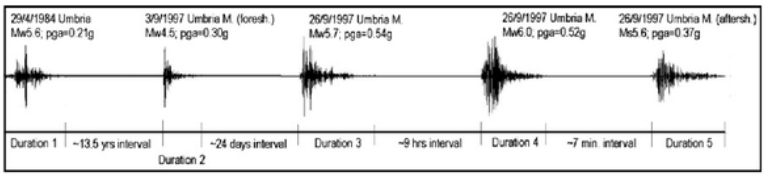

Fig. 1. Example of repeated earthquake ground motions recorded from Norcera Umbra Station, Italy.

Table 1
Examples of repeated earthquake events around the world.

No.	Station	Dir.	Earthquake name	Date	Time	Mag.	PGA (g)	Source
1	LDEO C0375VO, Turkey	NS	Duzce	07/11/1999	16:57	M_W¼7.2	0.919	ESD
		NS	Duzce (aftershock)	12/11/1999	16:54	M_W¼4.9	0.352	ESD
		NS	Duzce (aftershock)	13/11/1999	00:54	M_S¼4.5	0.304	ESD
		NS	Duzce (aftershock)	19/11/1999	19:59	M_S¼4.4	0.595	ESD
2	Norcera Umbra, Italy	NS	Umbria	29/04/1984	05:02	M_W¼5.6	0.209	ESD
		NS	Umbria-Marche (foresh.)	03/09/1997	22:07	M_W¼4.5	0.295	ESD
		NS	Umbria-Marche	26/09/1997	00:33	M_W¼5.7	0.538	ESD
		NS	Umbria-Marche	26/09/1997	09:40	M_W¼6.0	0.524	ESD
		NS	Umbria-Marche (aftersh.)	26/09/1997	09:47	M_S¼5.6	0.372	ESD
3	Kalamata OTE Bldg., Greece	EW	Kalamata	13/09/1986	17:24	M_S¼6.2	0.240	ESD
		EW	Kalamata (aftershock)	15/09/1986	11:41	M_S¼5.4	0.240	ESD
4	IITR Berlongfer, India	NS	India-Burma Border, India	09/01/1990	18:51	M_S¼6.1	0.142	Cosmos
		NS	India-Burma Border, India	06/08/1988	00:36	M_S¼7.2	0.344	Cosmos
5	CHY080, Taiwan	EW	Chi-Chi	20/09/1999	17:47	M_W¼7.6	0.082	Cosmos
		EW	Chi-Chi (aftershock)	20/09/1999	18:03	M_W¼6.2	0.048	Cosmos
6	CSB19001 Jiashi, China	WE	Northwest China (foresh.)	05/04/1997	23:46	M_W¼5.9	0.233	Cosmos
		WE	Northwest China (foresh.)	06/04/1997	04:36	M_W¼5.9	0.144	Cosmos
		WE	Northwest China	11/04/1997	05:34	M_W¼6.1	0.273	Cosmos
		WE	Northwest China (aftersh.)	15/04/1997	18:19	M_W¼5.8	0.239	Cosmos
7	Nahanni, NWT, Sta.1, Canada	NS	Nahanni, NWT	23/12/1978	05:16	M_S¼6.9	0.975	Cosmos
		NS	Nahanni, NWT (aftersh.)	23/12/1978	05:48	M_S¼5.4	0.228	Cosmos
8	DGG Llolleo, Chile	NS	Valparaiso	03/03/1985	22:47	M_S¼7.8	0.712	Cosmos
		NS	Valparaiso (aftershock)	03/03/1985	23:38	M_S¼6.3	0.186	Cosmos
		NS	Valparaiso (aftershock)	08/04/1985	23:27	M_S¼5.0	0.204	Cosmos
9	Imperial Valley, Array 9, USA	SN	El Centro	19/05/1940	04:36	M_W¼6.9	0.348	Cosmos
		SN	Borrego Mountain	09/04/1968	02:28	M_W¼6.5	0.130	Cosmos
		EW	Imperial Valley	15/10/1979	23:16	M_W¼6.5	0.236	Cosmos
		EW	Imperial Valley (aftersh.)	15/10/1979	23:19	M_L¼5.0	0.189	Cosmos
10	Cedar Hill NA, Tarzana, USA	EW	Whittier Narrows	01/10/1987	14:42	M_W¼6.1	0.405	Cosmos
		EW	Northridge	17/01/1994	12:30	M_W¼6.7	1.778	Cosmos
		EW	Northridge (aftershock)	20/03/1994	21:20	M_W¼5.3	0.372	Cosmos

NS¼North–South; EW¼East–West; WE¼West–East; SN¼South–North.
ESD¼European Strong-Motion Database [2].
Cosmos ¼ COSMOS Virtual Data Centre [3].

larger than those experienced by structures having non-degrading hysteresis model [9].

Very recently, Hatzigeorgiou and Liolios [10] have tried to address the deficiency of the MDOF issue. They examined two regular and two irregular reinforced concrete (RC) frames with specific behaviour factors and different dynamic characteristics. All those studies were carried out using ground motion characterized based on source-to-site distance only. In fact, the characteristic of near-field ground motion would be appropriately classified by its large pulse and permanent shifts contained in the motion. These pitfalls can increase the uncertainty of nonlinear dynamic analysis. Therefore, a more comprehensive study pertaining to repeated earthquake hazard on the system having a broad range of fundamental period of vibration and strengths, as well as an appropriate classification of ground motion, is needed. Furthermore, the pertinent literature had focused on SDOF or two-dimensional MDOF systems while this study examines for the first time three-dimensional frames under horizontal bi-directional seismic excitation. Consequently, the findings can be used as general insight and a tool in seismic evaluation. The present study aims to determine the effect of far-field repeated earthquakes on maximum story ductility demands and to develop empirical relationship of maximum story ductility demands on the inelastic RC frames due to repeated earthquakes.

2. Inelastic RC frame modelling

2.1. Simplified frames

Sixty moment-resisting frame systems in the form of generic frame models with three-dimensional multi-story single-bay configuration are evaluated in this study. They are developed based on the concept of Ruiz-Garcia and Miranda [11], previously proposed by Medina and Krawinkler [8]. These types of generic frames have been also used by Ibarra et al. [12] and extended to

multi-bays by Zareian and Krawinkler [13]. The simplified single-bay frame is adequate to represent the global seismic response (e.g., roof drift and maximum interstory drift) exhibited by regular multi-bay frame at different level of inelasticity [8,11,12]. The extension from two-dimensional to three-dimensional generic models was mainly intended to incorporate the bi-directional seismic action so that the near-field ground motion with forward directivity effect (FDE) can be rationally simulated because large pulse in FDE did not occur in both orthogonal directions [14]. In fact, many FDE motions having a large pulse in one direction were recorded in which the other component direction contained a motion with no large pulse as regular as the far-field ground motion.

The present study focuses on the regular geometric system using 3-, 6-, 12- and 18-story single-bay frame models (Fig. 2), which comply with Eurocode 8 [15] and ASCE 7-05 [16] as a regular horizontal and vertical system. The weight is lumped at the center of each story and arranged to remain constant at each story. The fundamental periods considered for the models are T_1 ¼0.45, 0.75, 1.26, and 1.71 s to reflect the common multi-story moment-resisting frame, particularly from 3 to 20 building stories [17]. The shape of the floors and roof are square with size of 7.2 ~ 7 m and with uniform column height of 3.6 m for all stories. To model the presence of a rigid slab, a rigid diaphragm assumption for the floor/roof is utilized. The columns and beams at each story have the same stiffness to reduce uncertainty and complexity in modelling and results assessment. Most building damages due to an earthquake occur at the member ends; hence, the inelasticity is modeled with flexural plastic hinges located at the member ends (full-hinge mechanism). More specifically, according to Fardis [18], the plastic hinge length can be estimated by the following relation

$$L_{pl} \approx 0.08 \sim L_s + a_{sl}(0.22 d_{bl} f_{yL}) \quad (f_{yL} \text{ in MPa}) \qquad (1)$$

where L_s is the member length, L_{pl} is the plastic hinge length, a_{sl} is a zero-one variable (with a_{sl}¼1 if slippage of longitudinal bars from the anchorage zone beyond the end section is possible, and a_{sl}¼0 if slippage is not possible) and d_{bl} the mean tension bar diameter. For the concrete frames under consideration, the above equation leads to $L_{pl} \approx 0.10 L_s$ and for this reason it can be assumed that L_{pl} 10%L_s. The P-delta effect is considered in the current work. A 5% Rayleigh damping ratio is used at the first mode and the mode where 90% of mass participation is attained. The use of such low damping ratio is common for moment-resisting frames as regulated in many codes (e.g., Eurocode 8 and ASCE 7-05). Moreover, to avoid inaccurate estimate of displacements, apparent when the Rayleigh damping is mixed with lumped plasticity model adopted for the plastic hinge at member ends [19], a practical approach of using the Rayleigh damping according to by Zareian and Medina [20] is used in the current study.

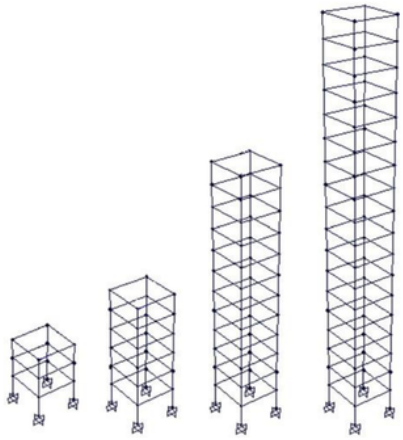

Fig. 2. Three-dimensional generic frame models representing 3-, 6-, 12-, and 18-story single-bay reinforced concrete frames.

2.2. Stiffness and strength distributions

The stiffness distribution used for the models is classified as regular stiffness according to ASCE 7-05, which means that the difference between the stiffness of adjacent stories is less than 60% of the story above or less than 70% of the average stiffness of the three stories above. This condition complies with Eurocode 8 as regular stiffness as well. The models are designed to exhibit the first-mode elastic deflected shape to be more realistic. Therefore, we used the ratio of the stiffness of all beams at the mid-height story of the frame to the sum of the stiffness of all columns at the same story based on the empirical relationship proposed by Miranda and Taghavi [21]. The stiffness distribution is tuned so that the variation of lateral stiffness along the height of the structure follows parabolic variations [22]. To have a more realistic simulation, the present study selects the decreasing stepwise distribution of lateral stiffness based on the resulting parabolic variation, and this lateral stiffness changes for every three stories. The dynamic characteristic of the models is listed in Table 2.

Four types of ductility-related behaviour factor q, namely, 1.5, 2, 4, and 6, are considered. This is done because most earthquake-resistant building designs using Eurocode 8 for moment-resisting frame have behaviour factors within the range of $1.5 \le q \le 4$ for medium ductility (denoted as DCM in Eurocode 8) and within the range of $4 \le q \le 6$ [18] for high ductility (DCH). The definition of the flexural plastic hinge is in line with the selected q using linear elastic analysis. The q factor is defined as the ratio of the ground motion intensity $S_e(T_1)/g$ to the design lateral force in the structure F_b divided by the weight of the structure W, as follows:

$$q = \frac{S_e(T_1) g}{F_b / W} \qquad (2)$$

This definition is also employed by others, including Medina and Krawinkler [8], Ruiz-Garcia and Miranda [11], and Zareian and Krawinkler [13]. Behaviour factor q affects the following modal seismic action $S_d(T)$

$$S_d(T) = S_e(T) / q \qquad (3)$$

where $S_d(T)$ is the modal seismic action taken from the design spectrum response acceleration at period T, $S_e(T)$ denotes the elastic response spectrum at period T, and q is equal to q_o times the overstrength (denoted by a_u/a_1 in Eurocode 8). In the present paper, the maximum flexural bending moment is selected as the strength parameter of the member, which is obtained from the linear elastic static lateral method using horizontal force F_i derived from F_b. This strength value is assigned as the yield moment to the hinge location in a generic frame. To adopt a strong column–weak beam mechanism in an earthquake resistant system, strength ratios equal to 1.3 between columns and beams are considered ($\Sigma M_b \ge 1.3 \Sigma M_{col}$), as suggested by Eurocode 8,

Table 2
Fundamental period of vibration $T_{1,2}$, third-mode period of vibration T_3, and normalized modal participation factor $MPF_{1,2}$, obtained for each model.

N	$T_{1,2}$ (s)	T_3 (s)	$MPF_{1,2}$
3	0.45	0.23	1.23
6	0.75	0.37	1.34
12	1.26	0.56	1.42
18	1.71	0.62	1.41

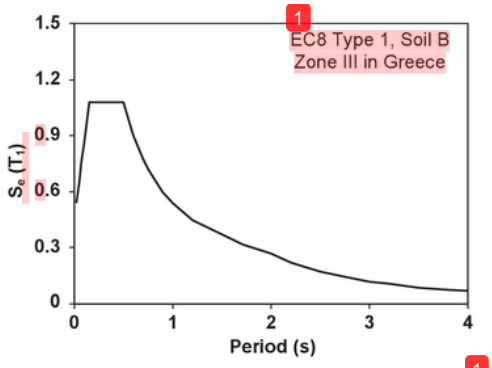

Fig. 3. Elastic spectrum acceleration of Eurocode 8 with 5% damping ratio for Type 1 and Soil B at Zone III of Greece.

in obtaining the height-wise strength distribution. The overstrength is also uniformly added with a factor of 1.3 of the available strength to represent the overstrength regulated in Eurocode 8 for real multi-story multi-bay structures. The strength is then tuned, and the mechanism is checked using pushover analysis by examining the plastic hinge progress. However, adjusting the system so that all beams will experience plastic hinges earlier than any column before the entire system collapses is neither realistic nor possible [13].

F_h is defined from ordinate design spectrum at period T_1 of the Type 1 spectrum of Eurocode 8 for Soil B condition. The elastic spectrum acceleration used in the present work with peak ground acceleration (PGA) a_g¼ 0.36 g is shown in Fig. 3. Soil B is selected because majority of available records in the European Strong Motion Database (40.8%) are sourced from stiff soil (Soil B) as discussed by Iervolino et al. [23]. a_g is based on a 475-year return period of earthquake that reflects the condition of Seismic Zone III in Greece. Greece represents the highest seismic region in Europe, along with Turkey and Italy, whereas Zone III is the zone with highest seismicity in Greece. The model is assumed to represent ordinary building, and hence, it has an importance factor equal to 1.0.

2.3. Plastic hinge and backbone curve

The plastic hinge is represented by a moment–rotation relationship, modelled using a lumped plasticity model. To simulate the cyclic behaviour of RC members in plastic hinge under load reversals, the modified-Takeda hysteresis rule is employed (Fig. 4), where the unloading and reloading parameters (a¼0.3 and b¼ 0.6) for the beam and column members are identical, as suggested by Fardis [24]. The backbone curve proposed by Zaerian and Krawinkler [13] is used, as shown by the thin line in Fig. 4. The yield rotation γ_y of a member is obtained by the ratio of M_y to elastic rotation stiffness (K_0¼ 6EI/L).

Plastic rotation capacity mostly affects the collapse capacity of the ductile system [12]. In an RC system, this parameter is mainly governed by the loss of confinement of the concrete core or onset of rebar buckling [25]. To represent the capacity of general RC structures, the current work employs the moment–rotation capacities of the RC beam–column members within the capacity range suggested by Haselton et al. [26] because their suggested capacity is based on the evaluation and calibration of the database from experimental testing of RC members, largely dominated by the data studied by Panagiotakos and Fardis [25]. To reflect the low, medium, and high rotation capacities of the RC members, the current work used plastic rotation capacity γ_p, namely, 0.02, 0.04, and 0.06, as proposed by Zareian and Krawinkler [13]. To the best of the authors' knowledge, the test data for the calibration of M_q/M_y and post-capping rotation γ_{pc} are insufficient because these

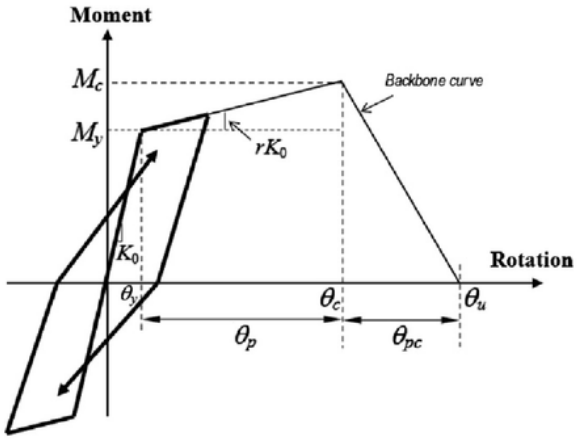

Fig. 4. Modified-Takeda hysteresis and backbone curve.

parameters are relatively new. Therefore, γ_{pc} is assumed to be equal to 0.06 based on the average value of γ_{pc} used in the Zareian and Krawinkler's study, whereas the ratio of M_q/M_y is assumed to be 1.13, as suggested by FEMA-P695 [27]. The post-yield stiffness ratio r is estimated based on M_y, capping moment, M_c, K_0, γ_y, and ductility of plastic rotation capacity $\mu_{y,c}$, as shown in Fig. 4.

Cyclic strength degradation can significantly increase the peak displacement demands of structures, particularly for short period of structures. The peak displacement demands are very sensitive to the changes of yield strength [28]. Therefore, the present study considers the strength degradation of the member based on rotation ductility from Zareian and Krawinkler's [13] backbone curve, developed based on the hysteresis rule proposed by Ibarra et al. [12].

In the current work, the parameters of r_K and $\mathbb{W}_c$ are introduced in order to characterize the stiffness and capacity of ductility of the global system, respectively. The ratio of global post-yield stiffness to elastic stiffness r_K of a model and the ratio of story ductility to global ductility capacities $\mathbb{W}_c$ of a model are defined using nonlinear static analysis. It is used as the inelastic properties of the considered concrete frame, which were governed by the fundamental period, behaviour factor, and rotation capacity of member. After regressing r_K of 60 models having varies T_1, q, and γ_p, the following expression is used to characterize the global stiffness of the considered models in the present work.

$$r_K = 10^{-0.132T_1^3 - 0.901\log(q) - 11.252\gamma_p - 1.290} \quad (4)$$

Eq. (4) has coefficient of determination, denoted by R^2, and standard deviation of error in log-normal distribution, denoted as S_{err}, of 0.972 and 0.072, respectively. The relationship explains that γ_p governs r_K compares with T_1 and q. The trend also clearly shows that as γ_p increases r_K decreases, a trend similar to that in the Zareian and Krawinkler study [13]. Only r_K with the range of 0–3% is evaluated in the current work. Moreover, the ratio of ductility capacity of the models represented by the ratio of story to global ductility capacity $\mathbb{W}_c$ is introduced to relate the maximum global ductility (based on roof displacement) with the maximum story ductility (based on interstory drift) capacity. The following empirical relationship of $\mathbb{W}_c$ reflects the ratio of ductility capacity of the 60 models, based on regression analysis (R^2 ¼ 0.983; S_{err} ¼ 0.028).

$$\mathbb{W}_c = 10^{0.513T_1^3 - 0.971T_1^2 - 0.406T_1^{-1} - 0.046Log(r_K) + 1.037} \quad (5)$$

The aforesaid relationship excludes q and γ_p since both have negligible effects on $\mathbb{W}_c$. It also clearly indicates that as T_1 increases,

W_c also increases. The models evaluated in the present work appear to have ratio of ductility capacity 1.2 ⌐W_c ⌐4.9.

3. Seismic input

3.1. Selection of ground motion record

In this work, twenty strong motion records have been examined, which have been downloaded from the European Strong Motion Database (ESD) [2], according to suggestions of Bommer and Acevedo [29]. These far-field earthquakes appear in Table 3 and are compatible with soil Type B of Eurocode 8 [23], i.e., compatible with the design process. The spectral acceleration at the fundamental period of a structure, denoted as $Sa(T_1)$, is utilized as the intensity measure of ground motion used in nonlinear response history analysis. The scaling process focuses on this intensity measure following the method proposed by Shome et al. [30], which is employed here due to its simplicity and accuracy [31].

3.2. Assembling synthetic repeated earthquakes

The main objective of this section is to provide with repeated earthquakes records, in order to examine their influence on

Table 3
Selected far-field earthquake ground motions from ESD.

No.	Date	Earthquake name	Mag. (Mw)	Dist. (km)	Station
1	09/15/1976	Friuli (aftersh.)	6.0	21	Breginj-Fabrika IGLI
2	09/15/1976	Friuli (aftersh.)	6.0	37	Kobarid-Osn.Skola
3	04/15/1979	Montenegro	6.9	25	Petrovac-Hotel Olivia
4	04/15/1979	Montenegro	6.9	24	Ulcinj-Hotel Olimpic
5	05/24/1979	Montenegro (aftersh.)	6.2	33	Bar-Skupstina Opstine
6	05/24/1979	Montenegro (aftersh.)	6.2	22	Kotor-Zovod
7	11/23/1980	Campano Lucano	6.9	43	Brienza
8	11/23/1980	Campano Lucano	6.9	48	Mercato San Severino
9	03/19/1983	Heraklio	5.6	40	Heraklio-Prefecture
10	10/16/1988	Kyllini	5.9	36	Armaliada-OTE Building
11	06/15/1991	Racha (aftersh.)	6.0	40	Iri
12	10/14/1997	Umbria-Marche (aftersh.)	5.6	24	Nocera Umbra
13	08/17/1999	Izmit	7.6	73	Goynuk-Devlet Hastanesi
14	09/07/1999	Athens/Ano Liosia	6.6	20	Athens 2, Chalandri District
15	06/27/1998	Adana-Ceyhan	6.3	80	Mersin-Meteoroloji Mudurlugu
16	06/17/2000	South Iceland	6.5	21	Selsund
17	11/18/1997	Strophades	6.6	38	Zakynthos-OTE Building
18	06/21/2000	South Iceland (aftersh.)	6.4	21	Hella
19	11/12/1999	Duzce 1	7.2	31	LDEO Sta. C1061
20	11/12/1999	Duzce 1	7.2	26	LDEO Sta. D0531 WF

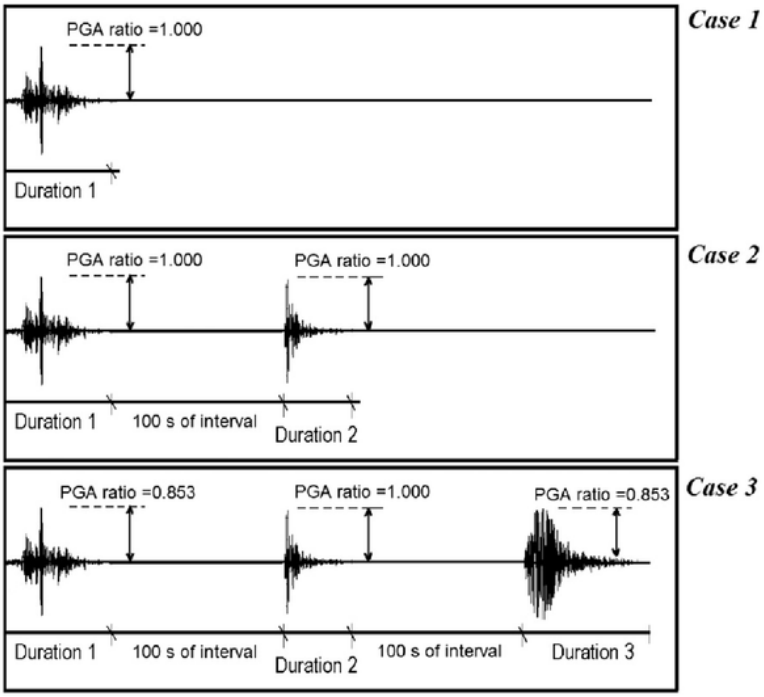

Fig. 5. Illustration of assembling the ground motion to generate synthetic repeated earthquakes.

structural behaviour, e.g., damage accumulation, in comparison with the corresponding single earthquakes. Up to now, the existent research [1,10,11] is limited to two-dimensional frames with seismic excitation in one (horizontal) direction only. In the present work, the repeated earthquakes are presented in a form of combination of the bi-directional ground motion with single, double, and triple events. Due to lack of real seismic sequences records, this paper examines only artificial sequences, where they have been generated by a rational combination of real single events. The assembly method is obtained from the study of Hatzigeorgiou and Beskos [5]. To the best of the authors' knowledge, no other practical method is found related to this issue. In this method, the amplitude ratio of the assembled ground motion is scaled based on the PGA ratio, as shown in Fig. 5, governed by the magnitude of consecutive earthquakes sourced from the same seismic region and recorded at the same site. The PGA ratio was derived using the ratio of empirical attenuation functions, which vary in magnitude [5]. The examined cases of double and triple seismic events appear to be realistic scenarios of multiply earthquakes and have been based on the findings of recognized research works on Engineering Seismology, such as the works of Gutenberg and Richter [30] and Joyner and Boore [31]. For more information, the reader can consult Refs. [5–7,10]. Thus, three types of amplitude ratios of assembled ground motion was used in the present paper, i.e., single earthquake event (mainshock only) with PGA amplitude ratio of (1.000, 0.000, 0.000) as GM Case 1, double earthquake events (foreshock–mainshock or mainshock–aftershock) with PGA amplitude ratio of (1.000, 1.000, 0.000) as GM Case 2, and triple earthquake events (foreshock–mainshock–aftershock) with PGA amplitude ratio of (0.853, 1.000, 0.853) as GM Case 3. An interval motion with zero amplitude of acceleration and 100 s duration was inserted between two consecutive ground motions. This interval is absolutely enough to achieve the state of rest of any ordinary multistory building after vibration due to inherent damping, as suggested by Hatzigeorgiou [7]. Each of the earthquake events is applied for GM Case 1 or single-event earthquake. For GM Cases 2 and 3, repeated earthquakes are assembled using different earthquake events randomly added to GM Case 1.

4. Result and discussion

The story ductility demand, defined as the mean value of maximum interstory drift from nonlinear time history analysis normalized by interstory yield from nonlinear static analysis, i.e., $\mu_s = d_{max}/d_y$, is used as the engineering demand parameter in the present paper. Figs. 6 and 7 show the trend of mean story ductility demand μ_s along the height under repeated earthquakes GM Cases 1, 2, and 3. For shorter system period, i.e., 3-story model in Fig. 6, the maximum story ductility demand $\mu_{s,max}$ due to GM Cases 1, 2, and 3 tends to appear at the top story. This is also true in the case of the 6-story model with q o2 in Fig. 6. This maximum demand then migrates to the bottom story as the strength decreases and as the building becomes taller. For taller models, all of $\mu_{s,max}$ due to GM Cases 1, 2, and 3 are situated at the bottom story, regardless of the type of behaviour factor and ground motion (Fig. 7), which means that the dispersion of $\mu_{s,max}$ of inelastic structures induced by repeated earthquakes of GM Cases 2 and 3 follows the same trend as that of GM Case 1. The influence of repeated earthquakes on the dispersion of $\mu_{s,max}$ is negligible. A similar trend was also found for the interstory drift on the 3- and 8-story RC frame models used by Hatzigeorgiou and Liolios [10] in evaluating the effect of repeated earthquakes. Using a different type of material (i.e., steel) and hysteresis rule, Ruiz-Garcia and Negrete-Manriquez [32] indicated that the story drift in the 4-, 8-, and 12-story inelastic models performed with the same trend as well. These two studies supported the aforesaid findings that mentioned that repeated earthquakes did not affect the dispersion of $\mu_{s,max}$ along the height. In general, the relative

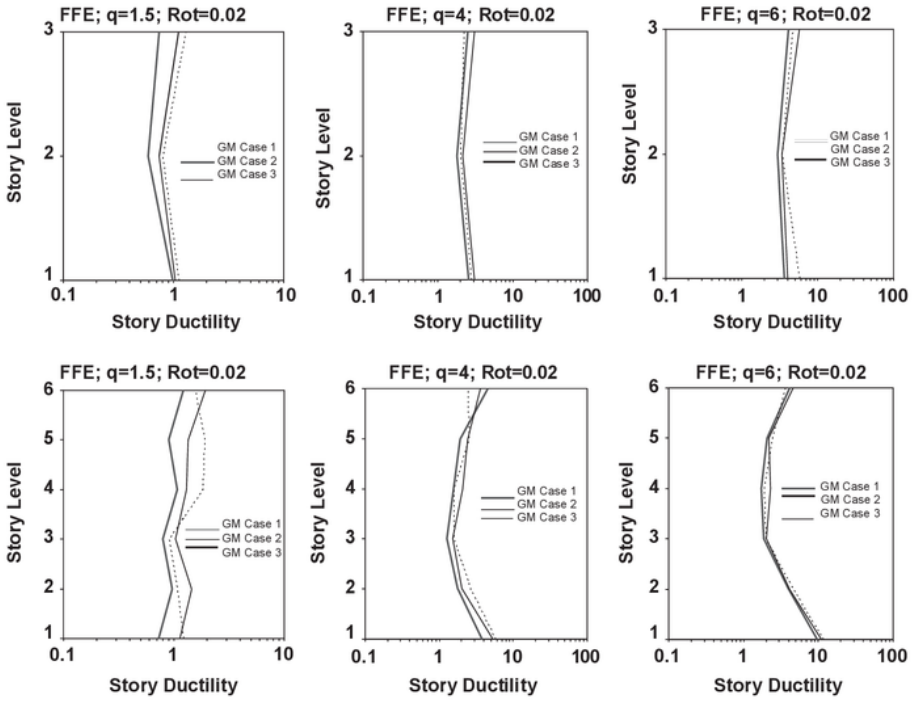

Fig. 6. Story ductility demands of 3- and 6-story inelastic concrete frames affected by repeated GM Cases 1, 2, and 3.

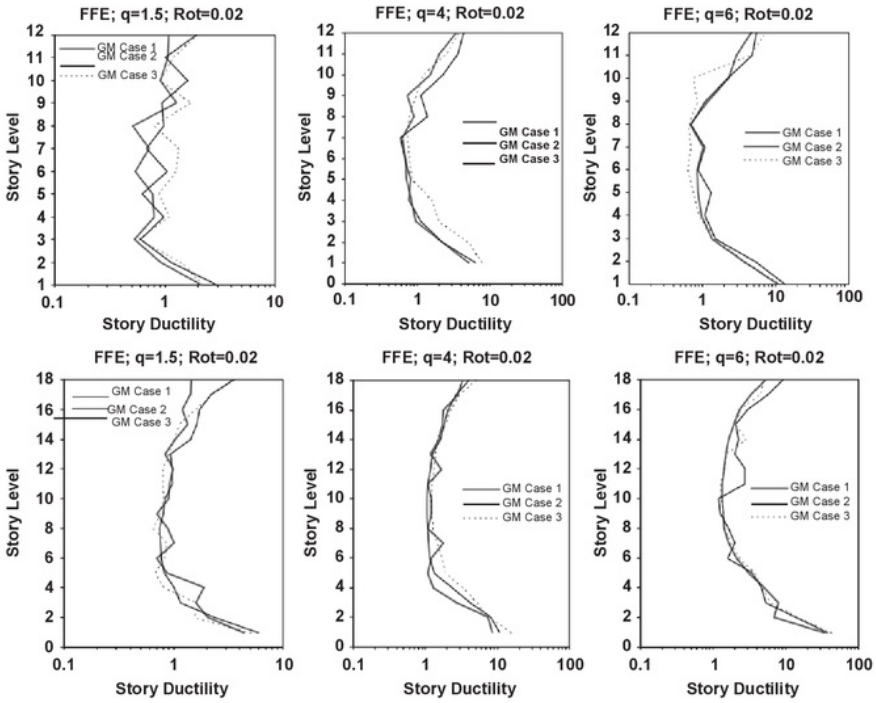

Fig. 7. Story ductility demands of 12- and 18-story inelastic concrete frames affected by repeated earthquake GM Cases 1, 2, and 3.

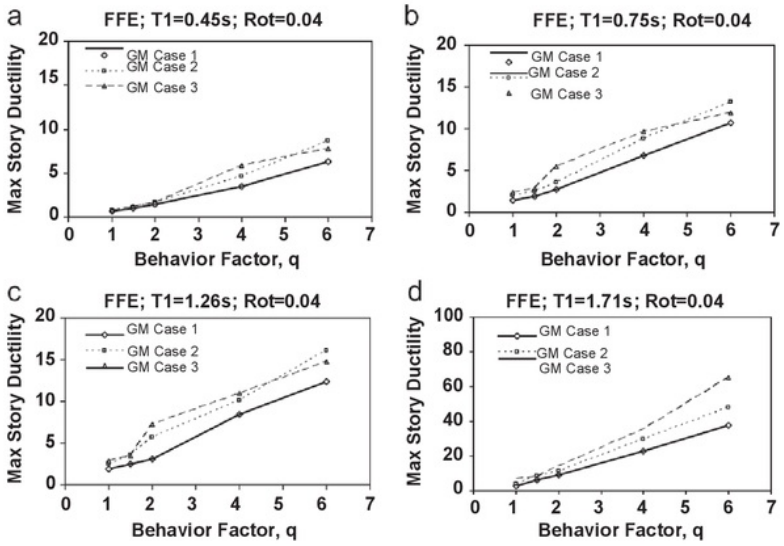

Fig. 8. Maximum story ductility demand of 3-, 6-, 12-, and 18-story inelastic concrete frames with 0.04 plastic rotation capacity due to repeated earthquakes.

increment of μ_s on the system due to repeated GM Case 2 or 3 tends to decrease as the behaviour factor increases. This trend is clearly evident as the number of story of the models (or fundamental period) increases, particularly on the 6- and 12-story models, as shown in Figs. 6 and 7. This is not the case, however, for all stories along the height.

The maximum story ductility demand of the considered inelastic concrete structures is shown as a function of behaviour factor in Fig. 8. The behaviour factor evidently affects the increment of maximum story ductility demands. An increase of behaviour factor tends to raise the relative increment of $\mu_{s,max}$, denoted as A_{r-sm}, regardless of the type of ground motions and fundamental period. Although in a few cases GM Case 2 is found dominant, i.e., models with $T_1 \approx 1.71$ s and $q = 6$, repeated earthquake GM Case 3 generally produces greater influence on A_{r-sm} than that of GM Case 2 for all types of ground motions. Moreover, the effect of repeated earthquakes on $\mu_{s,max}$ of models having $q \leq 2$ tends to be small and can be neglected. Only $\mu_{s,max}$ on structures with high q (i.e., $q = 4$ and 6) are affected by the presence of repeated earthquakes.

Table 4
$A_{r-\mu sm}$ on the models with average plastic rotation capacity and behaviour factor 1.5 ☛ q ☛6 induced by repeated earthquakes.

Models	Repeated GM case	q¼ 1.5	q¼ 2	q¼ 4	q¼ 6
3-story model (T_1 ¼0.45 s)	GM case 2	1.2	1.2	1.4	1.4
	GM case 3	1.3	1.2	1.4	1.3
6-story model (T_1 ¼0.75 s)	GM Case 2	1.5	1.3	1.3	1.1
	GM Case 3	1.7	1.9	1.4	1.1
12-story model (T_1 ¼ 1.26 s)	GM Case 2	1.4	1.6	1.2	1.3
	GM Case 3	1.3	1.8	1.3	1.1
18-story model (T_1 ¼ 1.71 s)	GM Case 2	1.5	1.4	1.2	1.2
	GM Case 3	1.5	1.7	1.6	1.5

$A_{r-\mu sm}$ on the models with fundamental period 0.45 ☛ T_1 ☛1.71 s (or systems having from 3 to 18 number of stories) with average plastic rotation capacity and qZ1.5 is listed in Table 4. On average, GM Case 3 propagates an increment of $\mu_{s,max}$ on the considered concrete frames 16% larger than GM Case 2. $A_{r-\mu sm}$, regardless of GM Case 2 or 3, are found within the ranges from 1.2 to 1.6 and from 1.1 to 1.5 for the system designed with DCM (q¼ 4) and DCH (q ¼6), respectively. In the system with DCM and DCH, the gaps of $A_{r-\mu sm}$ between GM Cases 3 and 2 reaches 19.2% and 12.8%, respectively. Therefore, the maximum story ductility on the system with DCM can be increased higher than the system with DCH when repeated earthquakes are propagated.

To the best of the authors' knowledge, similar studies that evaluated maximum story ductility demand on various types of fundamental period of vibration, plastic rotation capacity, and behaviour factors are not available yet. Therefore, comparison of maximum story ductility is difficult to make. Nevertheless, Hatzigeorgiou and Liolios [10] and Ruiz-Garcia and Negrete-Manriquez [32] studied the effect of repeated earthquakes on few models. The former focused on the roof ductility of 3- and 8-story regular RC frames having q ¼ 3.9. Their study graphically explained that the maximum interstory drift on the 8-story RC frame with T_1¼1.23 s increased from 1.4 to 1.75 times due to repeated earthquakes, meaning that the maximum story ductility of that structure increased in the same range of values due to repeated earthquakes. Ruiz-Garcia and Negrete-Manriquez [32] evaluated 3- and 8-story inelastic structures (T_1¼1.23 and 1.95 s) under real and synthetic repeated earthquakes. Their study graphically demonstrated that the increment of maximum interstory drift reached about 1.23 and 1.14 when synthetic earthquake induced the models at T_1 ¼ 1.23 and 1.95 s, respectively. There was no information pertaining to the behaviour factor they have used in their article. Therefore, the average maximum story ductility demand of the system having high ductile system, i.e., q¼4 to 6, were used, and the resulting increment of about 1.43 was due to the repeated near-field earthquake for system at T_1¼1.26 s. This finding is reasonable because the Ruiz-Garcia and Negrete-Manriquez's findings were based on ground motions having pulse and having slightly shorter fundamental period than the current study. The maximum interstory drifts on the model considered in Hatzigeorgiou and Liolios [10] and Ruiz-Garcia and Negrete-Manriquez [32] appeared in the lower stories, which well agreed with the current study.

4.1. *Predicting maximum story ductility demand*

It is well-known, e.g., from Refs. [5–7,10], that multiple earthquakes leads to increased deformation demands in comparison with the corresponding single events. The main objective of this section is to provide with empirical relations to estimate the maximum story ductility demands, $\mu_{s,max}$, for sequential strong ground motions. These empirical relations will be proposed for all the examined cases of Section 3.2.

First, one must define which variables were statistically significant to the dependent variable. Thus, applying sensitivity analysis it is found that the fundamental period (or equivalently the number of floors) and behaviour factor, strongly affect $\mu_{s,max}$ when repeated earthquakes occur. Two nonlinear structural parameters were also incorporated: the ratio of post-yield stiffness r_K, and the ratio of roof ductility to maximum story ductility capacities μ_c. The parameter r_K reflects the stiffness condition of the system in linear and nonlinear states, and reflects that the building becomes more flexible when r_K decreases. The value of P-delta that affects the system can also be explained by this parameter because the P-delta effect on the ratio of post-yield stiffness increases as the height of the building increases.

The nonlinear multiple regression analysis was performed to obtain regression parameters. The empirical formulas used to estimate the mean maximum story ductility demand, denoted by $\mu_{s,j}$, are shown in the following. The subscript j indicates the case of repeated earthquakes, which is from 1 to 3 for repeated GM Cases 1, 2, and 3, respectively. These can be predicted as follows:

$$\ln(\mu_{s,1}) = 0.761\ln(T_1) + 0.877\ln(q) + 0.112\ln(r_K^{-0.4}) - 0.300 \quad (6)$$

$$\ln(\mu_{s,2T_1}) = 0.785\ln(T_1) + 0.826\ln(q) + 0.501\ln(r_K^{-0.25}) - 0.893 \quad (7)$$

$$\ln(\mu_{s,3}) = 0.720\ln(T_1) + 0.610\ln(q) + 1.843\ln(r_K^{-0.15}) - 2.822 \quad (8)$$

where R^2 of these relationships are found to be 0.987, 0.988, and 0.974, respectively. Standard deviation of error, denoted by S_{err}, for Eqs. (6)–(8) are found to be 0.124, 0.126, and 0.184, respectively. Eqs. (6)–(8) were ones of the simplest equations which better described the numerical data following downward and upward concave curves after testing hundreds of mathematical equations. For the system induced by seismic repetition GM Case 2 or 3, $\mu_{s,j}$, can be estimated with the relationship in Eq. (9) with R^2 ¼ 0.979 and S_{err} ¼ 0.166, as follows:

$$\ln(\mu_{s,2-3}) = 0.726\ln(T_1) + 0.659\ln(q) + 1.774\ln(r_K^{-0.15}) - 2.694 \quad (9)$$

The efficiency of Eqs. (6)–(9) is shown in Fig. 9 where the proposed model results are compared with their counterparts from 'exact' dynamic inelastic analyses. In general, the diagonally scattered data appears in the range of $\mu_{s,j}$4 20 for all GM Cases, which is inevitable, especially at higher ductility level. It is due to the reason of selected range of behaviour factor and the P-delta effect of long-period RC models. Nevertheless, it is evident in any case that the results from predicted model obtained from this study are in good agreement based on R^2, S_{err}, F-sig ratio, and the scatter plot of correlation between prediction model and results obtained from the dynamic inelastic analyses. Therefore, by using Eqs. (6)–(9) the effect of repeated earthquakes on $\mu_{s,max}$ of reinforced concrete frame building in form of $A_{r-\mu sm}$ ¼ $\mu_{s,(j=1)}$/ $\mu_{s,1}$ can be predicted directly. These equations are valid only within the range considered in the present study.

4.2. *Case studies using the prediction formulas*

This section presents practical case studies in implementing the prediction formulas for the RC frame models, published by Hatzigeorgiou and Liolios [10]. Their models have been selected because they have been designed for the same region (Europe) covered in the present study. Likewise, they used these models to assess repeated earthquakes.

The models consist of 3- and 8-story moment-resisting RC frames, which represent low and medium-rise RC structures having fundamental period of vibration T_1 equal to 0.621 and 1.280 s, respectively. Both models have three equal bays with a

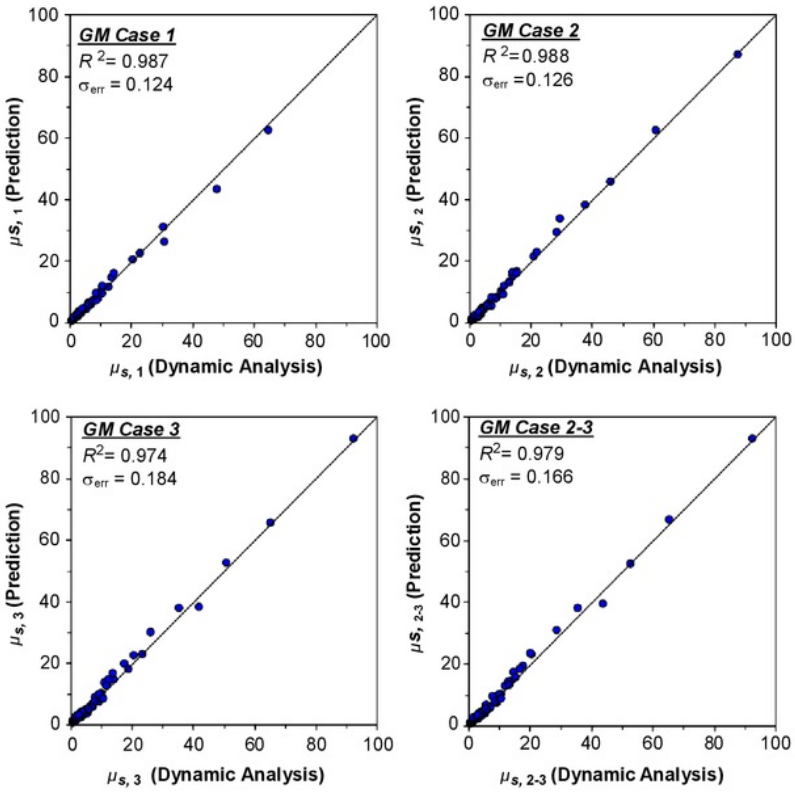

Fig. 9. Comparison of prediction model with analytical result of the mean maximum story ductility demand of inelastic concrete frames due to repeated earthquakes.

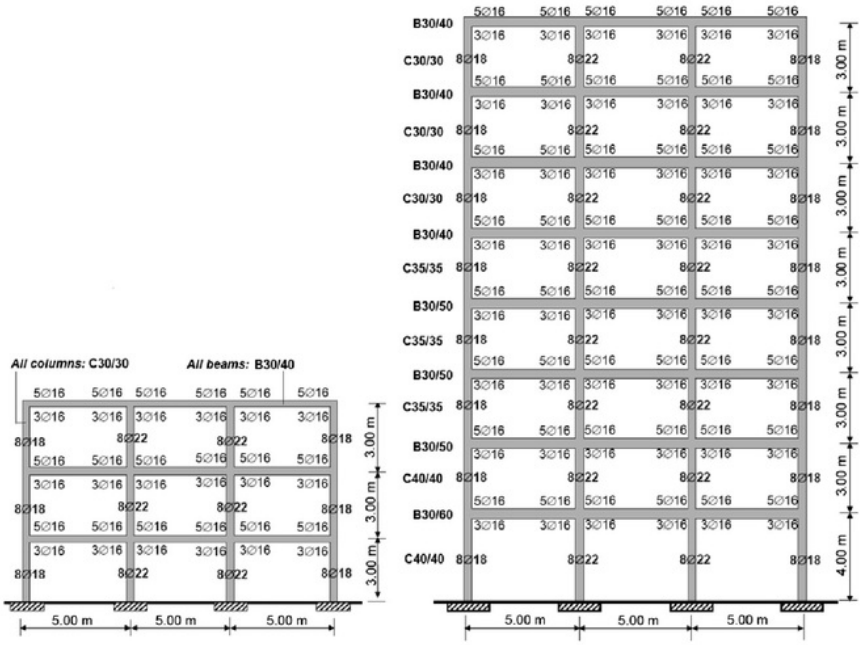

Fig. 10. Three- and eight-story moment-resisting concrete frames [10].

total length of 15 m, and all typical floor-to-floor heights are equal to 3.0 m, except for the first floor of the 8-story buildings whose height was equal to 4.0 m. The illustration of the models is shown in Fig. 10. The examined models, according to Eurocode 8 [15], are built on Class B soil located in Greece, a high-seismicity region of Europe. The model also considers both gravity and seismic loads,

Table 5
Selected far-field earthquake ground motion from ESD for the case studies.

No.	Date	Earthquake name	Mag. (*Mw*)	Epi. (km)	Station	Dir.
1	03/19/1983	Heraklio	5.6	40	Heraklio-Prefecture	EW
2	03/19/1983	Heraklio	5.6	40	Heraklio-Prefecture	NS
3	09/07/1999	Athens, Ano Liosia	6.6	20	Athens 2, Chalandri District	N126
4	09/07/1999	Athens, Ano Liosia	6.6	20	Athens 2, Chalandri District	N36
5	11/18/1997	Strofades	6.6	38	Zakynthos-OTE Building	140
6	11/18/1997	Strofades	6.6	38	Zakynthos-OTE Building	230

Table 6
Assembled ground motions as synthetic repeated earthquakes for the case studies.

GM no.	GM Case 1	GM Case 2	GM Case 3
1	GM No. 1	GM No.1–GM No.2	GM No.4–GM No.1–GM No.2
2	GM No. 3	GM No.3–GM No.4	GM No.6–GM No.3–GM No.4
3	GM No. 5	GM No.5–GM No.6	GM No.2–GM No.5–GM No.6

Table 7
Dynamic characteristics of 3- and 8-story frames.

	3-story model			8-story model		
	Mode 1	Mode 2	Mode 3	Mode 1	Mode 2	Mode 3
T_1 (s)	0.621	0.197	0.138	1.280	0.492	0.271
MPF	0.781	0.075	0.021	0.823	0.189	0.049

where a design PGA of 0.2 g is assumed. The dead loads (excluding self-weight) is equal to 20 kN/m, whereas the live load is 10 kN/m. Both loads are applied on the beams. Rigid diaphragm is assumed for all floors to represent the action of concrete slabs.

Both models have been designed for DCM class according to Eurocode 8, which has behaviour factor q¼ 3.9. The effective moments of inertia I_{ef} were considered in the design, namely, I_{ef}¼ 0.5 I_g for the beams and I_{ef}¼ 0.9 I_g for the columns, where I_g is the moment of inertia of the corresponding cross section. The concrete compressive strength (concrete grade C20) is assumed to be 20 MPa, whereas the yield strength for both longitudinal and transverse reinforcements is 500 MPa (steel grade S500). The reinforcement arrangement can be seen in Fig. 10. The elastic and shear moduli of concrete are assumed equal to 2.885 ~ 10^4 and 1.202 ~ 10^4 MPa, respectively.

For practical purposes, the models were induced by three ground motions, and thus, the maximum response is considered as the final result. The selected ground motion is presented in Table 5, taken from ESD that originally occurred in Greece. These ground motions were assembled within the same type of ground motion to generate the repeated earthquakes. The combination of assembled ground motions is presented in Table 6.

The results of eigenvalue analysis, i.e., fundamental period of vibration T_1 and mass participation factor *MPF*, are presented in Table 7. Based on pushover analysis, the global post-yield stiffness ratio r_K was found equal to 0.003442 for the 3-story model. Using the empirical formula given in Eq. (4), r_K was found to be equal to 0.004963, based on the result of T_1 in Table 7, plastic rotation capacity y_p¼ 0.04, and behaviour factor q¼ 3.9. The selection of y_p¼ 0.04 was based on assumption that RC members are well-detailed to avoid the loss of confinement of the concrete core or onset of rebar buckling [33]. The yield displacement was found to be equal to 0.0450 m, whereas the yield interstory drifts were equal to 0.0153, 0.0170, and 0.0127 for the first, second, and third stories, respectively. The ultimate displacement was equal to 0.573 m, whereas the ultimate interstory drifts were equal to 0.363, 0.154, and 0.018 for the first, second, and third stories, respectively. Therefore, the ductility capacity $\mathbb{W}_c$¼ 1.863 from the aforesaid results, which is in good agreement with 1.728 obtained from $\mathbb{W}_c$ of Eq. (5).

The global post-yield stiffness ratio r_K was found to be equal to 0.001926 for the 8-story model based on the pushover analysis. Using the empirical formula given in Eq. (4), r_K was equal to 0.002822. The yield and ultimate displacements were found to be equal to 0.071 and 0.821 m, whereas the maximum yield and ultimate interstory drifts were equal to 0.0164 and 0.427 m, respectively. Using these findings, the ratio of ductility capacities of the 8-story model was equal to $\mathbb{W}_c$¼2.251, in good agreement with 2.099 obtained from $\mathbb{W}_c$ of Eq. (5).

The story ductility results of the 3- and 8-story models indicate the extreme drift that occurs at the lower part. Although few cases indicate that GM Case 2 governed, most of GM Case 3 produced the maximum drift result. For the 8-story model, GM Case 3 governed all ground motions. The comparison of the analytical and prediction findings of the maximum story ductility demands for each case of repeated earthquakes (Table 6) is presented in Table 8. It is evident that very good agreement is achieved between the analytical results from dynamic inelastic analyses and the proposed empirical relations (Eqs. (6)–(8)). The relative increment of maximum story ductility demands due to repeated earthquakes is listed in Table 9. The bold values indicate the maximum analysis results from the three ground motions used. Furthermore, Table 9 shows that the prediction relationships can, in general, provide a very close estimation of the relative increment of maximum story ductility demands of the considered concrete frames excited by repeated earthquakes. Therefore, the empirical formulas produced by the current study in estimating the effect of repeated earthquakes can be used in seismic evaluation of buildings.

5. Conclusions

The present work explains the effect of repeated earthquakes on the story ductility demand of inelastic concrete frames. It concludes that the maximum story ductility demand of structures under consideration is found to be significantly affected by repeated earthquakes. However, the effect of repeated earthquakes on the maximum story ductility demand of models having behaviour factor of q ⌜2 tends to be small and can be neglected. The maximum story ductility demand on the structures induced by repeated earthquakes tends to appear in the upper level for a short structure, i.e., 3-story model, with low behaviour factor. This maximum demand then migrates to the bottom story as behaviour factor increases. For taller models, i.e., 6-, 12-, and 18-story models, all the maximum story ductility demands due to repeated earthquake GM Cases 1, 2, and 3 are situated at the bottom story, regardless of the type of behaviour factor. This finding means that the influence of repeated earthquakes on the dispersion of maximum story ductility demands is negligible.

Table 8
Comparison of the analytical and prediction findings for $m_{s,j}$.

GM No.	3-story			8-story		
	GM Case 1	GM Case 2	GM Case 3	GM Case 1	GM Case 2	GM Case 3
1	3.65	5.37	5.54	9.54	11.37	12.81
2	4.37	5.76	5.90	8.98	11.23	13.84
3	4.22	5.16	5.51	8.77	11.70	12.17
Prediction (Relative error—%)	4.33 (0.92)	5.72 (0.69)	5.75 (2.54)	9.52 (0.21)	13.45 (14.9)	13.90 (0.43)

Table 9
Comparison of the analytical and prediction findings for A_{r-max}.

GM No.	3-story		8-story	
	GM Case 2	GM Case 3	GM Case 2	GM Case 3
1	1.47	1.52	1.19	1.34
2	1.32	1.35	1.25	1.54
3	1.22	1.31	1.32	1.39
Prediction	1.32	1.33	1.41	1.46

On average, repeated earthquake GM Cases 2 and 3 increase the maximum story ductility demand up to 1.4 times higher than GM Case 1. On average, repeated earthquakes make the relative increment of maximum story ductility demand reach 1.4 and 1.3 times for DCM and DCH behaviour factors, respectively. In such cases, the relative increment of maximum story ductility demand due to repeated earthquake GM Cases 2 and 3 tends to decrease as behaviour factor increases. This trend is clearly evident as the number of story of the models (or fundamental period) increases, particularly in the 6- and 12-story models. These conclude that concrete frames designed with DCM have experienced higher relative increment of maximum story ductility demand than those with DCH behaviour factor when repeated earthquakes exhibited.

In the current paper, the empirical relationship used to predict the maximum story ductility demand of inelastic concrete structures under consideration affected by repeated earthquakes is also proposed. The applicability of the prediction formula is evaluated using 3- and 8-story RC buildings designed using European Code provisions. The result of relative increment of the maximum story ductility demand due to repeated earthquakes based on nonlinear analysis shows very good agreement with the predicted result.

The aforementioned conclusions appear to be new findings in the examined topic since none work in the past had not considered the effect of multiple earthquakes on the maximum story ductility demands. Furthermore, all the pertinent research works examined either SDOF systems or two-dimensional MDOF systems, while this work examines for the first time three-dimensional frames under bi-directional horizontal seismic excitation.

Finally, it should be noted that some uncovered, pertinent research topics need further study. For example the proposed method is limited to three-dimensional symmetric frames while asymmetric structures with intense torsional response can also be examined. Furthermore, other critical parameters, e.g., the roof ductility demands can also be investigated. Additionally, the response of three-dimensional frames under real seismic sequences can also be considered. All these topics are under investigation by the authors and will be presented in an oncoming research paper.

Acknowledgements

Authors are thankful to Mohd. Irwan Adiyanto, Mohd. Zulham Affandi Mohd Zahid, Mohd. Khairi Azuan Muhammad, Sabila Ahmad Basir, and Syafrina Mayang Sari for their supports during the study. The present study was supported by Research University Grant (1001/PAWAM/814115) sponsored by Universiti Sains Malaysia whereby the second author as the main investigator. The study of the first author were mainly supported by the Fellowship and Student Grant provided by Universiti Sains Malaysia and complemented by funds from Universitas Muhammadiyah Sumatera Utara. These supports are much appreciated.

References

[1] Amadio C, Fragiacomo M, Rajgelj S. The effects of repeated earthquake ground motions on the non linear response of SDOF systems. Earthquake Engineering and Structural Dynamics 2003;32:291–308.
[2] Ambraseys N, Smit P, Sigbjörnsson R, Suhadolc P, Margaris P. Internet-Site for European Strong-motion Data. /http://www.isesd.cv.ic.ac.uk, EVR1-CT-1999-40008, in, European Commission, Directorate-General XII, Environmental and Climate Programme, Bruxelles, Belgium, 2001.
[3] COSMOS Virtual Data Centre. /http://db.cosmos-eq.org/scripts/earthquakes.plx [accessed: 2010/10/10].
[4] Muria Vila D, Toro Jaramillo AM. Effects of several events recorded at a building founded on soft soil. In: 11th European Conference on Earthquake Engineering, Paris, 1998.
[5] Hatzigeorgiou GD, Beskos DE. Inelastic displacement ratios for SDOF structures subjected to repeated earthquakes. Engineering Structures 2009;31:2744–55.
[6] Hatzigeorgiou GD. Behavior factors for nonlinear structures subjected to multiple near-fault earthquakes. Computers and Structures 2010;88:309–21.
[7] Hatzigeorgiou GD. Ductility demand spectra for multiple near- and far-fault earthquakes. Soil Dynamics and Earthquake Engineering 2010;30:170–83.
[8] Medina RA, Krawinkler H. Seismic demands for non-deteriorating frame structures and their dependence on ground motions. Report no. TR 144, John Blume Earthquake Engineering Centre, Stanford University, 2003.
[9] Ruiz-García J, Miranda E. Residual displacement ratios for assessment of existing structures. Earthquake Engineering and Structural Dynamics 2006;35:315–36.
[10] Hatzigeorgiou GD, Liolios AA. Nonlinear behaviour of RC frames under repeated strong ground motions. Soil Dynamics and Earthquake Engineering 2010;30:1010–25.
[11] Ruiz-Garcia J, Miranda E. Performance-based assessment of existing structures accounting for residual displacements. Report no. 153, John A. Blume Earthquake Engineering Center, Stanford University, Stanford, 2005.
[12] Ibarra L, H. Krawinkler H. Global collapse of frame structures under seismic excitations. Report no. 2005/06, Pacific Earthquake Engineering Research Center, University of California at Berkeley, Berkeley, 2005.
[13] Zareian F, Krawinkler H. Simplified performance-based earthquake engineering. Report no. 169, John A. Blume Earthquake Engineering Center, Stanford University, Stanford, 2009.
[14] Bray JD, Rodriguez-Marek A. Characterization of forward-directivity ground motions in the near-fault region. Soil Dynamics and Earthquake Engineering 2004;24:815–28.
[15] CEN. Eurocode 8: Design of structures for earthquake resistance. Part 1: General rules, seismic actions and rules for buildings. European Committee for Standardization, Brussels, 2004.
[16] American Society of Civil Engineers (ASCE). Minimum design loads for buildings and other structures. ASCE/SEI 7-05. Reston, VA: ASCE; 2005.
[17] Goel RK, Chopra AK. Period formulas for moment-resisting frame buildings. Journal of Structural Engineering 1997;123:1454–61.

[18] Fardis MN. Seismic design, assessment and retrofitting of concrete buildings: based on EN-Eurocode 8. New York: Springer; 2009.
[19] Hall JF. Problems encountered from the use (or misuse) of Rayleigh damping. Earthquake Engineering and Structural Dynamic 2005;35:525–45.
[20] Zareian F, Medina RA. A practical method for proper modeling of structural damping in inelastic plane structural systems. Computers and Structures 2010;88:45–53.
[21] Miranda E, Taghavi S. Approximate floor acceleration demands in multistory buildings. I: Formulation. Journal of Structural Engineering ASCE 2005;131:203–11.
[22] Miranda E, Reyes CJ. Approximate lateral drift demands in multistory buildings with nonuniform stiffness. Journal of Structural Engineering ASCE 2002;128:840–9.
[23] Iervolino I, Maddaloni G, Cosenza E. Eurocode 8 compliant real record sets for seismic analysis of structures. Journal of Earthquake Engineering 2008;12:54–90.
[24] Fardis MN. Guidelines for displacement-based design of buildings and bridges. Pavia: IUSS Press; 2007.
[25] Panagiotakos TB, Fardis MN. Deformations of reinforced concrete members at yielding and ultimate. ACI Structural Journal 2001;98:135–48.
[26] Haselton CB, Liel AB, Lange ST, Deierlein GG. Beam-column element model calibrated for predicting flexural response leading to global collapse of RC frame buildings. Report no. 2007/03. Pacific Earthquake Engineering Research Centre, University of California at Berkeley, Berkeley, 2007.
[27] Applied Technology Council (ATC). Quantification of building seismic performance factors, FEMA P695. Washington, DC: Federal Emergency Management Agency; 2009.
[28] Applied Technology Council (ATC). Effects of strength and stiffness degradation on the seismic response of structural systems, FEMA P440A. Washington, DC: Federal Emergency Management Agency; 2009.
[29] Bommer JJ, Acevedo AB. The use of real earthquake accelerograms as input to dynamic analysis. Journal of Earthquake Engineering 2004;8:43–91.
[30] Shome N, Cornell CA, Bazzurro P, Carballo JE. Earthquakes, records, and nonlinear responses. Earthquake Spectra 1998;14:469–500.
[31] Giovenale P, Cornell CA, Esteva L. Comparing the adequacy of alternative ground motion intensity measures for the estimation of structural responses. Earthquake Engineering and Structural Dynamics 2004;33:951–79.
[32] Ruiz-García J, Negrete-Manriquez JC. Evaluation of drift demands in existing steel frames under as-recorded far-field and near-fault mainshock-aftershock seismic sequences. Engineering Structures 2011;33:621–34.
[33] ASCE. Seismic rehabilitation of existing buildings (ASCE/SEI 41-06). American Society of Civil Engineers (ASCE); 2007.

SDEE-Faisal-etal-2013

ORIGINALITY REPORT

21%	%	%	21%
SIMILARITY INDEX	INTERNET SOURCES	PUBLICATIONS	STUDENT PAPERS

PRIMARY SOURCES

1	Submitted to Universiti Sains Malaysia Student Paper	10%
2	Submitted to Universiti Teknologi MARA Student Paper	7%
3	Submitted to Michigan Technological University Student Paper	1%
4	Submitted to Hellenic Open University Student Paper	<1%
5	Submitted to University College London Student Paper	<1%
6	Submitted to Imperial College of Science, Technology and Medicine Student Paper	<1%
7	Submitted to University of Hong Kong Student Paper	<1%
8	Submitted to University of Leeds Student Paper	<1%
9	Submitted to CSU, San Jose State University	

	Student Paper	<1%
10	Submitted to City University Student Paper	<1%
11	Submitted to University of Canterbury Student Paper	<1%
12	Submitted to University of Osijek Student Paper	<1%
13	Submitted to Grand Canyon University Student Paper	<1%
14	Submitted to Middle East Technical University Student Paper	<1%
15	Submitted to University of Arizona Student Paper	<1%
16	Submitted to Vietnam Maritime University Student Paper	<1%
17	Submitted to University of Bristol Student Paper	<1%
18	Submitted to Universiti Putra Malaysia Student Paper	<1%
19	Submitted to Chulalongkorn University Student Paper	<1%

Exclude quotes	Off	Exclude matches	Off
Exclude bibliography	Off		